Proc. Natl. Acad. Sci. USA
Vol. 89, pp. 10154–10158, November 1992
Biophysics

Time-resolved circularly polarized protein phosphorescence

(optical activity/circularly polarized phosphorescence/glucose-6-phosphate dehydrogenase/horse liver alcohol dehydrogenase)

JOSEPH A. SCHAUERTE*†, DUNCAN G. STEEL*‡, AND ARI GAFNI*†

*Institute of Gerontology, ‡Department of Physics and Electrical Engineering, and †Department of Biological Chemistry, University of Michigan, Ann Arbor, MI 48109

Communicated by Paul D. Boyer, July 6, 1992

ABSTRACT **The existence of circular polarization in room-temperature protein phosphorescence is demonstrated, and time-resolved circularly polarized phosphorescence (TR-CPP) is used to characterize unique tryptophan environments in multitryptophan proteins. Circularly polarized luminescence studies provide information regarding the excited state chirality of a lumiphore which can be used to extract sensitive structural information. It is shown by time resolving the circular polarization that it is possible to correlate the excited state chirality with unique decay components in a multiexponential phosphorescence decay profile. The present study presents a concurrent analysis of room-temperature time-resolved phosphorescence and TR-CPP of bacterial glucose-6-phosphate dehydrogenase as well as those of horse liver alcohol dehydrogenase. Only one of the two tryptophan residues per subunit of dimeric alcohol dehydrogenase is believed to phosphoresce, while the dimeric glucose-6-phosphate dehydrogenase has eight tryptophan residues per subunit and shows a corresponding complexity in its phosphorescence decay profile. The anisotropy factor [$g_{em} = \Delta I/(I_{total}/2)$; $\Delta I = I_{left\ circular} - I_{right\ circular}$] for alcohol dehydrogenase is time independent, suggesting a unique excited state chirality. The phosphorescence decay of glucose-6-phosphate dehydrogenase can be well fitted with four exponential terms of 4, 23, 76, and 142 msec, and the TR-CPP of this enzyme shows a strong time dependence that can be resolved into four individual time-independent anisotropy factors of −4.0, −2.1, +6.5, and +6.9 ($\times 10^{-3}$), each respectively associated with one of the four lifetime components. These results demonstrate how the use of TR-CPP can facilitate the study of proteins with multiple lumiphores.**

The widespread occurrence of room-temperature protein phosphorescence (1–3) has generated a great deal of recent interest due to the possibility of extracting new information regarding protein structure and dynamics. Phosphorescence studies yield information on the environment of the triplet state of a chromophore, in contrast to the environment of the singlet state in fluorescence studies. The conformational and dynamic properties of protein structure are reflected in the lifetime of the singlet and triplet states of a chromophore, which provide complementary information regarding the environment of the chromophore. The great sensitivity of the long-lived triplet state to slight changes in its environment gives studies based on measurements of phosphorescence lifetime the potential to detect conformational changes and other dynamic processes which occur on the time scale of milliseconds to seconds.

Circularly polarized luminescence (CPL) is a reflection of the chirality of the excited chromophore and has been used extensively to obtain structural information which is complementary to that derived from circular dichroism spectroscopy for the ground state (for reviews see refs. 4–8). CPL reflects the differential emission of left and right circularly polarized light by a sample and is conventionally expressed by the anisotropy factor g_{em} [$g_{em} = \Delta I/(I_{total}/2)$; $\Delta I = I_{left\ circular} - I_{right\ circular}$]. For absorption and emission, the respective g values may be related to the corresponding magnetic and electric dipole matrix elements of the transition (4) by the following equations:

$$g_{ab} = \frac{\Delta\varepsilon}{\varepsilon} = \frac{\varepsilon_l - \varepsilon_r}{\varepsilon} = \frac{4\nu}{\nu_{kj}} \cdot \frac{R_{kj}}{|\langle j|\mu|k\rangle|^2}$$

and [1]

$$g_{em} = \frac{\Delta I}{\frac{1}{2}I} = \frac{(I_l - I_r)}{\frac{1}{2}(I_l + I_r)} = \frac{4\nu}{\nu_{jk}} \cdot \frac{R_{jk}}{|\langle k|\mu|j\rangle|^2},$$

where $R_{kj} = \mathrm{Im}\{\langle j|\mu|k\rangle \langle k|\mathbf{m}|j\rangle\}$, $\mu = e\Sigma_i r_i$, and $\mathbf{m} = (e/2mc)\cdot \Sigma_i r_i p_i$.

In the present work we demonstrate the existence of a circularly polarized component in the room-temperature phosphorescence of proteins in solution and use the time dependence of the polarization to provide information about the nature of the phosphorescent tryptophans. Time-resolved circularly polarized phosphorescence (TR-CPP) is used in the analysis of the room-temperature tryptophan phosphorescence of glucose-6-phosphate dehydrogenase (G6PDH) from *Leuconostoc mesenteroides*, liver alcohol dehydrogenase (LADH) from horses, and alkaline phosphatase (AP) from *Escherichia coli*.

G6PDH is a dimeric enzyme of 55 kDa per subunit containing eight tryptophan residues per subunit (9). Room-temperature phosphorescence has not previously been reported in this protein to our knowledge; however, our data show that the decay is characterized by multiexponential behavior. LADH is a dimeric enzyme of 40 kDa per subunit which contains two tryptophan residues per subunit (10); however, only one tryptophan in each subunit phosphoresces at room temperature (1). AP is a dimeric enzyme with a total molecular mass of 86 kDa and three tryptophan residues per subunit (11). However, earlier work showed that only Trp-109, which is not accessible to solvent (12), is phosphorescent (13, 14).

While TR-CPP has several potential applications as discussed below, this manuscript focuses on the use of this technique to provide additional information which we show facilitates the interpretation of complex multi-exponential luminescence decay data. The difficulty in interpreting such data resides in the uncertainty in assigning terms extracted from a nonlinear least-squares fit of a multi-exponential

The publication costs of this article were defrayed in part by page charge payment. This article must therefore be hereby marked "*advertisement*" in accordance with 18 U.S.C. §1734 solely to indicate this fact.

Abbreviations: CPL, circularly polarized luminescence; CPP, circularly polarized phosphorescence; TR-CPP, time-resolved CPP; G6PDH, glucose-6-phosphate dehydrogenase; LADH, liver alcohol dehydrogenase; AP, alkaline phosphatase; MCS, multichannel scaler.

decay to unique tryptophans or conformations (15). However, we demonstrate here that the additional information obtained from TR-CPP allows us to assign unique circular polarization factors to the individual decay components in a phosphorescence decay in a manner analogous to the use of decay-associated spectra (DAS) (16) for the identification of individual tryptophans in fluorescence studies. The additional information pertaining to the excited state chirality derived from TR-CPP enables a more precise interpretation of structural perturbations.

It is interesting to note that a time-resolved CPL approach has recently also been used to determine the optical activity of enantiomers in a racemic mixture by differential quenching of these enantiomers in the presence of chiral quenching agents (17–21). In these studies it was determined that quenching occurred by dynamic means and that the interconversion process can be followed.

For the detailed study of protein TR-CPP, we have developed instrumentation capable of determining g_{em} values as small as 10^{-4}, associated with lifetimes ranging from microseconds to seconds. This time range is of particular significance for the study of protein structure and dynamics because conformational transitions, as occur, for example, during binding or folding, take place on this time scale. It is therefore anticipated that TR-CPP will prove useful in studies of changes in the chiral environment due to protein interactions and will serve in studies of protein folding and assembly as well as ligand–protein association.

MATERIALS AND METHODS

All reagents and proteins were purchased from Sigma except horse LADH, which was purchased from Boehringer Mannheim. Samples were dialyzed against the appropriate buffer for 24 hr and then centrifuged to remove any precipitate. Enzyme activities were assayed according to established procedures (22–24) and protein purity was determined by sodium dodecyl sulfate/polyacrylamide gel electrophoresis (SDS/PAGE). Deoxygenation of samples was performed according to Englander *et al.* (25) by purging the sample with purified argon. One-centimeter cuvettes were used for data acquisition, and protein absorbances were approximately 0.1 to 0.2.

A block diagram of the instrumentation used to measure TR-CPP is presented in Fig. 1*A*. The instrument employs gated photon counting and a photoelastic modulator (Hinds International; model PEM-80) operating at 42 kHz which, in conjunction with a linear polarizer, modulates the circularly polarized component of the phosphorescence at the same frequency (Fig. 1*B*). A delay gate generator (Stanford Research; model 535) is timed to the reference output of the photoelastic modulator and establishes a gate of 6 μsec after a zero crossing trigger from the modulator. There are two gate pulses per period and each gate is centered about either the positive or the negative amplitude of the sine wave. The gates are used by a fast ECL (emitter-collector logic) "AND" logic unit (Paulus Engineering; Model AG1 Trigger Box) to switch the photomultiplier/discriminator output between two MCS cards (Ortec ACE-MCS).

A triggering pulse from the Q switch of the neodymium:yttrium–aluminum-garnet (Nd:YAG) laser used in sample excitation initiates a scan by the MCS cards with the modulator/gate generator/AND gate combination sequentially dividing each decay into the two MCS cards. An example of data obtained from a *single* laser shot is shown in Fig. 1*B*. Since the phase of the modulation of the photoelastic modulator determines whether right or left circularly polarized photons are transmitted preferentially, one of the MCS cards will have higher counts if the sample's emission contains a circularly polarized component. Since no correlation exists between the timing of the laser shots and the modulation, numerous uncorrelated laser excitations will eventually provide a smooth decay curve in each MCS card, as shown in our experimental data.

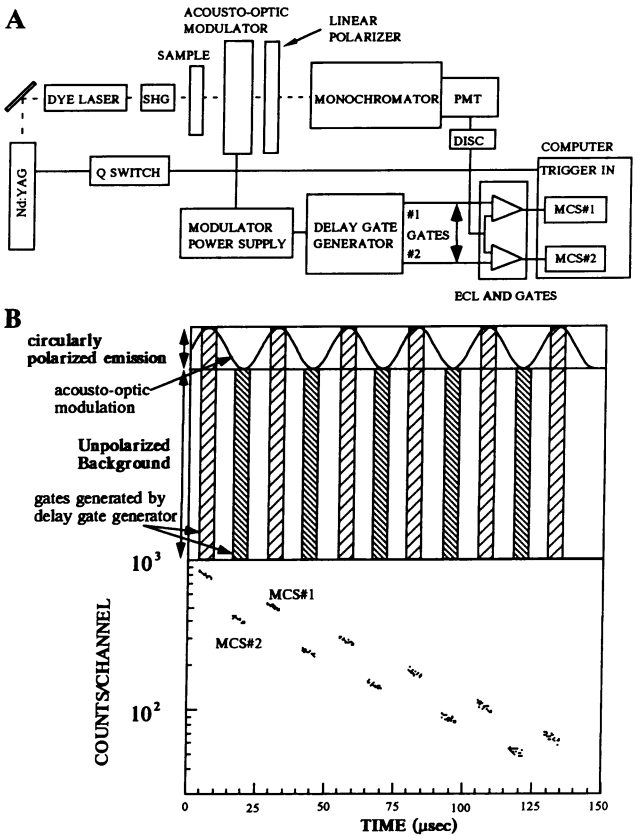

FIG. 1. (*A*) Block diagram of the instrumentation for TR-CPP. SHG, second harmonic generator; MCS, multichannel scaler; PMT, photomultiplier tube. The laser Q switch simultaneously triggers the multichannel scalers in the computer, and the gates generated from the modulator/delay gate generator enable the photomultiplier signal to be directed into either one of two MCS cards, depending upon the phase of the modulator, and to modulate right/left circularly polarized radiation. (*B*) Time-resolved gates associated with the modulation voltage of a photoelastic modulator allow for a discrimination between the transmission efficiency of right and left circularly polarized luminescence. Exaggerated schematic of data generated by gating a single decay profile into two separate MCS cards at the frequency of the photoelastic modulator. Since there is no correlation between excitation pulse and modulation phase, decay profiles accumulated over a large number of excitation pulses (>500) become smoothed. The maximum time resolution is 2 μsec, based on minimum dwell time of the MCSs.

Sample excitation for TR-CPP was by a Quanta-Ray DCR-11 Nd:YAG (135 mJ per pulse) pumping a Spectra-Physics PDL-3 dye laser using rhodamine 6G to obtain output at 560 nm. This output was frequency doubled (INRAD, Northvale, NJ; R6G potassium dihydrogen phosphate crystal) and filtered to excite the sample at 280 nm. The laser system was externally triggered with a repetition rate adjusted to allow the longest-lived decay component to decay at least 100-fold between pulses. A monochromator (Instruments-SA model HR-320) was used to select the emission wavelength. Residual excitation light from the emission beam was eliminated with 3 M potassium nitrite. The instrument was calibrated by introducing known amounts of circular polarization (26) into the steady-state luminescence of $TbCl_3$ excited by an argon laser (Spectra-Physics) at 488 nm.

Steady-state phosphorescence spectra are measured by integrating the total phosphorescence decay at a selected

emission wavelength, ignoring the counts in the first channel which are associated with the fluorescence, and repeating this procedure across the emission spectra. This approach differs from earlier *steady-state* measurements of CPL from fluorescence described by Steinberg and Gafni (26), using phase-sensitive detection, and later by Schippers *et al.* (27), using photon counting techniques.

The highest photon counting rates attainable by using a MCS are limited by the pulse-pair resolution of the electronics. With laser excitation, emission counting rates can be large enough to saturate the system and yield a nonlinear response (28). Peak counting rates were therefore limited by introducing neutral density filters in the excitation beam, reducing the extent of nonlinearity to less than 1%.

Since typical anisotropy factors in the emission are smaller than 10^{-3}, it is necessary to accumulate on the order of 10^9 total counts per MCS card, which in turn requires the use of over 10^4 laser shots. Special consideration must be given to the effect of extensive UV excitation on the phosphorescence decay characteristics of a protein even under deoxygenated conditions as used here. In general, several samples were exchanged to limit the total number of excitation pulses any sample receives.

The phosphorescence and TR-CPP were analyzed assuming that each phosphorescence decay component has a unique time-independent g_{em}. The analysis was done by using a Marquardt nonlinear least-squares procedure in which the data were fit to the following equation:

$$g_{em}(t) = \frac{\sum \alpha_i g_{em,i} e^{-t/\tau_i}}{\sum \alpha_i e^{-t/\tau_i}}, \quad [2]$$

where $\Sigma \alpha_i = 1$. The values used for α and τ are those derived from the total phosphorescence decay data. The total experimental decay profile was fit according to the appropriate photon counting statistics. The data were weighted by the variance $\sigma^2 = n$, where n is the number of counts in each channel. This assumption is valid for a large number of excitation pulses. The function $g_{em}(t)$ can be shown to have a variance $\sigma^2 = 2/n$, and therefore the theoretical fit was weighted accordingly.

RESULTS AND DISCUSSION

The demonstration that room-temperature phosphorescence is observable from extensively deoxygenated solutions of the majority of proteins (1–3) has spurred strong interest in this phenomenon, since the information obtained complements that derived from fluorescence. Tryptophan residues with long-lived (>1-msec) triplet states are believed to reside only in the hydrophobic interior of proteins, and their lifetimes reflect the rigidity (viscosity) of the residue's immediate environment. Hence, the wide range of decay times typical of protein phosphorescence reflects differences in local viscosity of the emitting tryptophans. In the case of singlet states, additional structural information is obtained by studies of the associated optical activity through circular dichroism and circularly polarized luminescence (4–8), which report on the chirality of the residue in either the ground state or the excited singlet state. CPP provides complementary information regarding the chirality of the triplet state. While CPP from several biological systems has been reported before (29), intrinsic protein CPP has proven to be more difficult to measure because the strong tryptophan fluorescence largely masks the relatively weak room-temperature phosphorescence. TR-CPP, on the other hand, enables one to reject the short-lived fluorescence signal and to extract the information on the triplet state chirality. Moreover, since as a rule different tryptophan residues in a protein have markedly different phosphorescence decay constants (though similar spectra), it should be possible to resolve their CPP spectra in a manner analogous to the resolution of protein fluorescence into the spectra of individual tryptophan residues by generating decay-associated spectra (16).

In this communication we describe the development and application of a sensitive instrument for the measurement of intrinsic TR-CPP of proteins in fluid solutions at room temperature on the millisecond time scale. Of the three proteins studied, the long-lived (>1-msec) phosphorescence decays of two (AP and LADH) have been previously shown to originate in single tryptophan residues [Trp-109 in AP (13) and Trp-314 in LADH (1)]. In accordance with this determination, we found the phosphorescence decay of AP to be well fit with a single exponential with a lifetime of 2.0 sec (see Table 1). Moreover, the TR-CPP of AP was time independent, with a g_{em} of -4.5×10^{-3} (data not shown). The exceptionally long decay time for AP phosphorescence is believed to reflect the great rigidity of the immediate environment of Trp-109. The time-invariant g_{em} supports the assertion that the tryptophan residue remains largely immobile during its excited triplet state lifetime. While this simplifying assumption is used in the analysis of the data presented below, it is clear that more experimental evidence is needed to decide whether this observation is generally true. More specifically, a time-invariant g_{em} may also be the result of fluctuations in structure on a time scale short compared with the triplet state lifetime, circumstances that would produce an averaged g_{em}. However, this seems unlikely, since the rigid environment surrounding a phosphorescing residue, believed to be a prerequisite for long-lived phosphorescence, would be expected to preclude substantial conformational changes in these domains during the triplet state lifetime needed to produce a time-averaged g_{em} value.

The phosphorescence decay kinetics of LADH have been previously reported to be monoexponential, provided oxygen is thoroughly removed from the solution (30). However, while the exceptionally long-lived phosphorescence obtained for LADH in the present study does attest to very efficient deoxygenation, we consistently observed multiexponential decay characteristics which could be well fit to three exponentials (see Fig. 2). Protein heterogeneity is not considered a likely explanation for the highly multiexponential decay, since the LADH samples used showed no impurity detectable within the 2% error in SDS/PAGE. Also, LADH enzyme

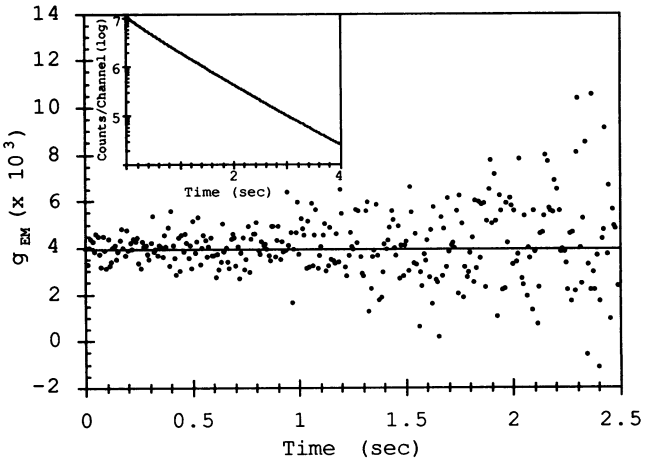

FIG. 2. Time-resolved g_{em} of LADH in 100 mM 3-(*N*-morpholino)propanesulfonic acid (Mops), pH 7.2. The sample was excited at 280 nm and phosphorescence was observed at 436 nm. The dwell time is 10.0 msec per channel. Results of least-squares fit are tabulated in Table 1, with a χ^2 of 1.4. (*Inset*) Phosphorescence decay profile of LADH.

activity was within experimental error of that reported by the supplier. The decay parameters, summarized in Table 1, show that the short decay component accounts for less than 4% of the phosphorescence, while the two long-lived components are responsible for over 96% of the emitted light. The fact that the lifetimes of the latter components differ by less than 30% may explain why the multiexponential decay behavior of LADH phosphorescence has escaped detection in previous studies, which lacked the extensive data acquisition employed here. The multiexponential decay characteristics are not the result of laser-induced degradation of the protein, as the pre-exponentials and lifetimes of the 550- and 790-msec components were uncorrelated with the amount of laser irradiation.

The TR-CPP profile of LADH (Fig. 2) shows a lack of time dependence for g_{em}, which supports the view that the phosphorescence originates in one tryptophan residue. When the coenzyme fragment adenosine diphosphoribose (ADPR) was bound to LADH, a monoexponential decay of 1.3 sec was observed with a time-independent g_{em} that was statistically indistinguishable from that of apo-LADH. It appears, therefore, that while the conformational changes in LADH involved in ADPR binding affect the rigidity of the Trp-314 environment and hence its phosphorescence decay rate, they leave the chirality of this residue unmodified. On the basis of this comparison with LADH/ADPR we assign the multiexponential decay of apo-LADH phosphorescence to conformational heterogeneity of this enzyme. The time-invariant g_{em} strongly suggests that the heterogeneity of LADH conformations alters the lifetime of the tryptophan through different local viscosities of the conformers but that the chirality of the environment of this residue's excited state is not affected.

Multiexponential phosphorescence decay kinetics were also revealed by the multitryptophan protein G6PDH from *L. mesenteroides*. The experimental data, displayed in Fig. 3*A*, show that the decay curve beyond 1 msec is well fit by four exponential components (pre-exponential terms and lifetimes listed in Table 1), with the third component contributing about 70% of the steady-state phosphorescence intensity, while less than 1% originates in the first component. It is important to note, however, that this is due to the short lifetime of this component and not to its presence in a small amount: the pre-exponential factor of 0.18 reflects the fact that this component does not represent a trace impurity. The multiexponential phosphorescence decay of G6PDH is not surprising, since this protein has eight tryptophan residues per subunit.

Fig. 3*B* shows the TR-CPP of G6PDH and reveals a strong time dependence for g_{em}. The emission anisotropy data were analyzed, assuming four decay components with lifetimes and amplitudes as derived from the phosphorescence decay curve (Fig. 3*A*). Each component is associated with a time-independent g_{em} to be determined by the analysis. While data analysis reveals an excellent fit of this model to the experimental data, this should not be taken as proof for the model used—i.e., the possibility cannot be dismissed that a smaller number of time-dependent g_{em} values could be used to generate the observed curve. It is important to note that even

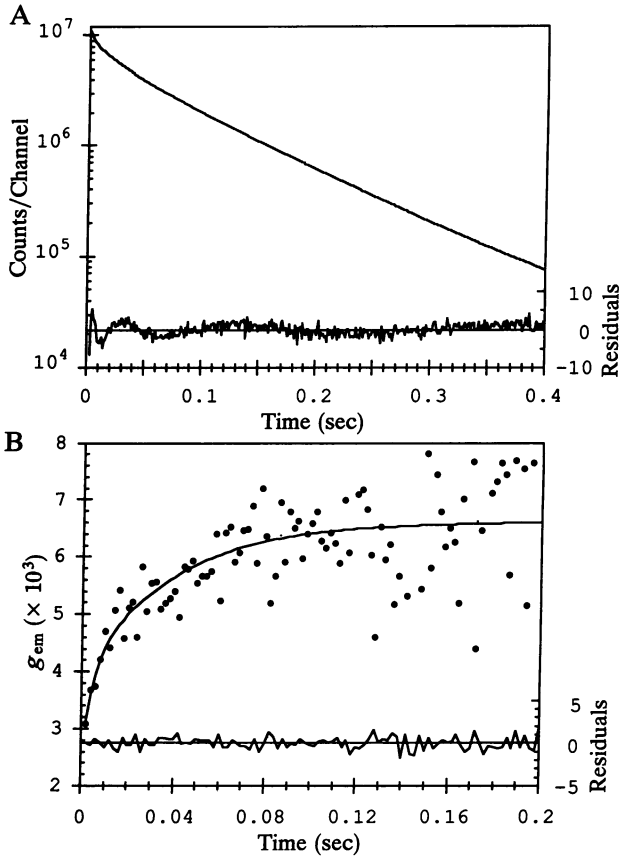

FIG. 3. (*A*) Phosphorescence decay profile of G6PDH in 100 mM Tris, pH 8.2, at 19°C. The sample was excited at 280 nm and the emission was detected at 436 nm with a dispersion of 9.6 nm. The dwell time is 1.0 msec per channel. Results of least-squares fit are tabulated in Table 1. Channels 2–450 are used for the analysis, yielding a χ^2 of 2.3. (*B*) Time-resolved g_{em} of G6PDH under the same conditions. Solid line represents theoretical fit according to Eq. 2 with time-invariant g_{em} (see Table 1) associated with each decay component. The residuals between theoretical fit and data are shown below g_{em}, with a χ^2 of 1.0 for the fit.

the assignment of individual phosphorescence decay components to specific tryptophan residues requires further consideration. This assumption is based on the bulk of experimental evidence obtained so far, which shows that tryptophan phosphorescence, unlike fluorescence, decays nearly monoexponentially. The data, however, are based on a small number of proteins with long phosphorescence lifetimes—i.e., proteins characterized by high rigidity in the vicinity of the residue, resulting in reduction of mobility.

We should note that we assumed that each g_{em} is uniquely associated with a single decay time and by implication a unique residue. It is possible, however, to imagine the presence of interresidue interactions such as energy transfer. Such coupling could result in the loss of correlation between the different g_{em} values and lifetimes. Also, the third and fourth g_{em} components of G6PDH have very similar values,

Table 1. Decay parameters obtained for phosphorescence and TR-CPP from AP, LADH, and G6PDH

Protein		α_1	τ_1, msec	α_2	τ_2, msec	α_3	τ_3, msec	α_4	τ_4, msec
AP		0.97 ± 0.00	1989.0 ± 1.0	0.03 ± 0.002	136.0 ± 14.0				
	$g_{em} \times 10^3$	−4.5 ± 0.2							
LADH		0.11 ± 0.014	178.0 ± 2.4	0.58 ± 0.015	539.0 ± 3.3	0.31 ± 0.033	792.0 ± 3.7		
	$g_{em} \times 10^3$	3.9 ± 0.1 (time-independent)							
G6PDH		0.18 ± 0.01	3.7 ± 0.05	0.23 ± 0.01	23.4 ± 0.2	0.52 ± 0.01	76.4 ± 0.4	0.07 ± 0.02	142.0 ± 2.0
	$g_{em} \times 10^3$	−4.0 ± 2.5		−2.1 ± 1.0		6.5 ± 0.2		6.9 ± 0.7	

All fits ignore phosphorescence below 1 msec.

as shown in Table 1. While this may be a coincidence, this similarity may reflect the fact that the two longest lifetimes are associated with the same tryptophan residue in two different conformations of the enzyme, as in the case of LADH.

The main conclusion from the above discussion is that the long-lived phosphorescence of G6PDH originates from three (possibly four) tryptophan residues, each associated with a distinct decay constant and a time-independent g_{em}. The decay constants are mostly affected by the rigidity of the environment of the residue, while the anisotropy factor reflects subtle structural details of the tryptophan domain. The information derived from these two parameters is therefore complementary and not redundant, and the two measurements can be used in conjunction to gain information on the number of emitting residues and to correlate distinct decay constants with individual residues.

The utility of TR-CPP in protein studies may be further enhanced by differentiating the response of individual tryptophan residues to external perturbing agents. For example, studies of dynamic quenching of G6PDH phosphorescence using triplet quenchers have shown that some of the chiral tryptophan residues are more susceptible to quenching (unpublished results).

The study of protein structure is obviously not limited to intrinsic tryptophan CPP. Several calcium-binding proteins have been shown to bind Tb^{3+} and emit circularly polarized luminescence after energy transfer from excited tyrosine residues (31–35). It is possible to show that subtle differences in metal ion binding site structures, which produce only minor differences in lifetimes of Tb^{3+}, can be resolved when the metal ions are in environments that exhibit different g_{em} values. Other phosphorescent probes such as benzophenone and anthracene that bind to proteins may prove beneficial in studies investigating unique chiral binding sites. Conversely, studies in which dynamic processes are reflected in alterations in the chirality during the excited state lifetime may provide additional new perspectives.

It is interesting to note that the g_{em} values observed for tryptophan phosphorescence in all three proteins studied here are approximately an order of magnitude larger than the values previously reported for the circular polarization of tryptophan fluorescence in a number of proteins (36). While the optical activity associated with weak electronic transitions is known to be enhanced, it should be noted that the triplet–singlet transition involved in phosphorescence is forbidden by the spin selection rule and is not, in general, associated with a weak oscillator strength. Hence if universal, this enhancement is presently not understood and would warrant investigation. From the experimental point of view the large g_{em} values obviously enhance the accuracy of the measurement, thus aiding in the identification of contributions from individual tryptophan residues to the spectrum.

In conclusion, this study demonstrates the existence of time-resolved circularly polarized intrinsic phosphorescence in the emission of proteins in solution at room temperature. The data were used to determine the uniqueness of the different phosphorescence decay times. However, the sensitivity of this technique to molecular conformation combined with the time range typical of protein phosphorescence (milliseconds to seconds) makes TR-CPP a powerful spectroscopic tool for the study of numerous reactions involving proteins.

This work is supported by Grant AG09761 from the National Institute on Aging and by the Office of Naval Research. Spectra-Physics generously provided the lasers.

1. Saviotti, M. L. & Galley, W. C. (1974) *Proc. Natl. Acad. Sci. USA* **71**, 4154–4158.
2. Vanderkooi, J. M., Calhoun, D. B. & Englander, S. W. (1987) *Science* **236**, 568–569.
3. Papp, S. & Vanderkooi, J. M. (1989) *Photochem. Photobiol.* **49**, 775–784.
4. Richardson, F. S. & Riehl, J. P. (1977) *Chem. Rev.* **77**, 773–792.
5. Steinberg, I. Z. (1978) *Methods Enzymol.* **49**, 179–199.
6. Riehl, J. P. & Richardson, F. S. (1986) *Chem. Rev.* **86**, 1–16.
7. Brittain, H. G. (1985) in *Molecular Luminescence Spectroscopy: Methods and Applications*, ed. Schulman, S. G. (Wiley, New York), pp. 583–620.
8. Brittain, H. G. (1987) *Photochem. Photobiol.* **46**, 1027–1034.
9. Levy, H. R. (1986) in *Glucose-6-Phosphate Dehydrogenase*, eds. Yoshida, A. & Beutler, E. (Academic, New York), pp. 279–299.
10. Eklund, H., Nordstrom, B., Zeppezauer, E., Soderlund, G., Ohlsson, I., Boiwe, T., Soderberg, B.-O., Tapia, O. & Branden, C.-I. (1976) *J. Mol. Biol.* **102**, 27–59.
11. Kim, E. E. & Wychoff, H. W. (1989) *Clin. Chim. Acta* **186**, 175–188.
12. Sowadski, J. M., Handschumacher, M., Krishna Murthy, H. M., Foster, B. A. & Wyckoff, H. W. (1985) *J. Mol. Biol.* **186**, 417–433.
13. Strambini, G. B. (1987) *Biophys. J.* **52**, 23–28.
14. Mersol, J. V., Steel, D. G. & Gafni, A. (1991) *Biochemistry* **30**, 668–675.
15. Siemiarczuk, A., Wagner, B. D. & Ware, W. R. (1990) *J. Phys. Chem.* **94**, 1661–1666.
16. Knutson, J. R., Walbridge, D. G. & Brand, L. (1982) *Biochemistry* **21**, 4671–4679.
17. Metcalf, D. H., Synder, S. W., Wu, S., Hilmes, G. L., Riehl, J. P., Demas, J. N. & Richardson, F. S. (1989) *Photochem. Photobiol.* **49**, 775–784.
18. Metcalf, D. H., Synder, S. W., Demas, J. N. & Richardson, F. S. (1990a) *J. Am. Chem. Soc.* **112**, 469–479.
19. Metcalf, D. H., Synder, S. W., Demas, J. N. & Richardson, F. S. (1990b) *J. Phys. Chem.* **94**, 7143–7153.
20. Reid, M. F. (1990) *J. Lumin.* **45**, 384–386.
21. Rexwinkel, R. B., Meskers, S. C. J., Riehl, J. P. & Dekkers, H. P. J. M. (1992) *J. Phys. Chem.* **96**, 1112–1120.
22. Vallee, B. L. & Hoch, F. L. (1955) *Proc. Natl. Acad. Sci. USA* **41**, 327–338.
23. Garen, A. & Levinthal, C. (1960) *Biochim. Biophys. Acta* **38**, 470–483.
24. Olive, C. & Levy, H. R. (1967) *Biochemistry* **6**, 730.
25. Englander, S. W., Calhoun, D. B. & Englander, J. J. (1987) *Anal. Biochem.* **161**, 300–306.
26. Steinberg, I. Z. & Gafni, A. (1972) *Rev. Sci. Instrum.* **43**, 409–413.
27. Schippers, P. H., van den Beukel, A. & Dekkers, H. P. J. M. (1982) *J. Phys. Sci. Instrum.* **15**, 945–950.
28. Loudon, R. (1973) *Quantum Theory of Light* (Clarendon, Oxford), p. 114.
29. Steinberg, N., Wachtel, E. J. & Gafni, A. (1982) *Biochemistry* **21**, 2573–2578.
30. Strambini, G. B. & Gonnelli, M. (1990) *Biochemistry* **29**, 196–203.
31. Burtnick, L. D. & Schaar, P. L. (1979) *FEBS Lett.* **97**, 166–170.
32. Brittain, H. G., Richardson, F. S. & Martin, R. B. (1976a) *Biochem. Biophys. Res. Commun.* **68**, 1013–1019.
33. Brittain, H. G., Richardson, F. S. & Martin, R. B. (1976b) *J. Am. Chem. Soc.* **98**, 8255–8260.
34. Kilhoffer, M.-C., Demaille, J. G. & Gerard, D. (1980a) *FEBS Lett.* **116**, 269–272.
35. Kilhoffer, M.-C., Demaille, J. G. & Gerard, D. (1980b) *FEBS Lett.* **120**, 99–103.
36. Steinberg, I. Z., Schlessinger, J. & Gafni, A. (1974) *Peptides, Polypeptides and Proteins*, eds. Blout, E. R., Bovey, E. A., Goodman, M. & Lotan, N. (Wiley, New York), pp. 351–369.